American Mineralogist, Volume 77, pages 296–302, 1992

Formation of fluid inclusions and etch tunnels in olivine at high pressure

TRACY N. TINGLE
Department of Geology, University of California, Davis, California 95616, U.S.A.
ED ROEDDER
Department of Earth and Planetary Science, Harvard University, Cambridge, Massachusetts 02138, U.S.A.
HARRY W. GREEN II
Department of Geology, University of California, Davis, California 95616, U.S.A.

ABSTRACT

Tubes, 3–10 μm in diameter and up to 3 mm long, and linear arrays of spherical and crystallographically faceted fluid inclusions, 5–35 μm in diameter, were produced in single crystals of San Carlos olivine (Fo_{89}) annealed in the presence of CO_2 and CO_2-H_2O fluids at 2–3 GPa and 1200–1400 °C in a piston-cylinder apparatus utilizing NaCl-BN sample assemblies. Experiments conducted under identical conditions in the same apparatus utilizing NaCl + pyrex + alumina sample assemblies did not produce tubes or fluid inclusions. Subsequent oxidation of one specimen to reveal the dislocation substructure showed that inclusions that can be traced to tubes in the process of necking down and linear inclusion arrays (representing healed tubes) are connected by single and multiple curvilinear dislocations. These observations suggest that the tubes formed on growth dislocations that existed in the olivine crystals prior to annealing. The formation of tubes is sensitive to chemical environment, and the growth rate of tubes is dependent on temperature. The tubes are interpreted to be etch tunnels, based on their similarity to etch tunnels produced in synthetic and natural quartz by HF etching and hydrothermal treatment. The most commonly accepted origin for etch tunnels in quartz is that growth dislocations segregate impurities (H or Al) that locally enhance the solubility of the crystal in the fluid. It appears that etch tunnels in olivine are produced by a similar mechanism.

INTRODUCTION

During the course of experiments to measure the solubility and diffusivity of C in San Carlos olivine by ^{14}C β-track autoradiography (Tingle et al., 1988), it was noted that some specimens annealed at high pressure (2–3 GPa) in the presence of CO_2 and CO_2-H_2O contained fluid-filled tubes and inclusions that clearly had not formed by crystal growth or by injection of fluid along fractures and subsequent diffusional crack healing. The tubes we have produced at high pressure are similar in many respects to etch tunnels produced by HF etching of natural and synthetic quartz (Nielsen and Foster, 1960; Hanyu, 1964; Carstens, 1968; Iwasaki, 1977; Folk et al., 1987; Folk, 1989). We have characterized these experimentally induced features to infer the mechanism of their formation and their relevance to geologic processes.

EXPERIMENTAL TECHNIQUES

Specimens and experimental procedures have been described in detail by Tingle et al. (1988) and are only briefly described here. Doubly polished plates cut from single crystals of gem-quality olivine (Fo_{89}) from San Carlos, Arizona, were cored to produce crystallographically oriented cylinders 2.2 mm od and 1.2–2.0 mm long whose flat ends were polished. Either graphite plugs with the same dimensions as the crystals or powdered olivine were placed above and below the crystals, and in most cases, Au or Mo foil separated the crystal from the graphite or powdered olivine. Two fluid sources (both enriched with ^{14}C) were employed; silver oxalate, which decomposes to metallic Ag and CO_2, or oxalic acid monohydrate, which decomposes to CO_2, H_2O, and H_2 in molar proportions 2:1:1, was weighed into the bottom of a Pt capsule and sealed (welded shut) with the specimens. The capsules were pressurized in a piston-cylinder apparatus, generally in NaCl-BN sample assemblies; a few experiments were conducted in NaCl + pyrex + alumina assemblies (see Fig. 1 of Tingle et al., 1988). As described by Tingle (1988), specimens with graphite plugs were retrieved after annealing at 2.0–3.0 GPa and 1200–1400 °C for up to 48 h with few or no cracks, using slow steady depressurization and quenching (≈200 MPa/min and 100 °C/min). Specimens with few or no cracks were removed from their capsules and examined by optical and scanning electron microscopy. Petrographic sections were prepared from all specimens. All specimens were exposed to Ilford K5 nuclear emulsions (25 μm thick on glass slides) as described by Tingle (1987) and Tingle et al. (1988) to record β particles emitted by ^{14}C.

0003–004X/92/0304–0296$02.00

Experimental results

Occurrence of tubes

Single crystals of San Carlos olivine annealed in the presence of CO_2 and CO_2-H_2O at 2.0 and 3.0 GPa, 1200–1400 °C for periods of 2 h to 2 weeks in NaCl + BN sample assemblies displayed tubes, 3–10 μm od and up to 3 mm long, and inclusions 5–35 μm od (Figs. 1, 2). Specimens that were quenched immediately after pressurization to 3.0 GPa and heating to 1200 °C (zero-time experiments) showed no inclusions or tubes. Significantly, tubes were not observed in specimens annealed in NaCl + pyrex + alumina sample assemblies. The most important difference between experiments performed in the two sample assemblies is probably the fugacities of the various fluid species; the f_{O_2} stabilized inside sealed Pt capsules by H_2 diffusion in the NaCl + BN and NaCl + pyrex + alumina assemblies has been estimated at 10^{-10} and 10^{-5} bars, respectively (Tingle et al., 1988). Although these estimates are subject to some uncertainty, it is clear that the NaCl + BN assemblies are considerably more reducing than the NaCl + pyrex + alumina assemblies (see also Wendlandt et al., 1983).

In almost all cases, the tubes penetrated from the bottom of the specimen upward, even in one specimen where the fluid source was placed at the top of the capsule. In addition, two specimens showed tubes penetrating inward from the circumference of the cylinder along a principal crystallographic direction (Fig. 2). Crystallographic control of tube penetration was observed in some specimens; in other specimens, the tubes penetrated in a radial pattern from the bottom. The β-track autoradiography demonstrates that tubes and inclusions contain ^{14}C.

Inclusions typically define linear arrays, which in many cases can be traced to tubes in the process of necking down (Fig. 1). In some specimens, individual inclusions displayed negative crystallographic facets (not shown). The distribution of tubes and inclusions is irregular; one part of a crystal may contain numerous tubes and inclusions, whereas another part of the same crystal may contain virtually none (Fig. 2). These tubes and inclusions cannot represent cracks formed during pressurization that subsequently healed at high temperature because they do not define two-dimensional arrays (surfaces). Second, special sample assemblies and procedures were developed (see Tingle, 1988) that allowed us to pressurize, anneal, and quench the relatively large olivine specimens without introducing cracks; tubes also developed in some of these crack-free specimens.

It appears that the growth rate of tubes scales with temperature, suggesting that growth of tubes, or some process related to their formation, is thermally activated (Fig. 3). Four experiments at 1200 °C lasting 46–54 h produced maximum tube lengths (inferred from the longest tube or linear array of fluid inclusions) ranging from 0.1 to 1.2 mm, and one experiment at 1400 °C lasting 2 h produced tubes 0.5 mm long (Table 1). Our limited data do not allow us to determine if the process is dependent on pressure or follows an Arrhenius relationship. Given that the experimental conditions for the four 1200 °C experiments were essentially identical, the variable tube lengths suggest that temperature and chemical environment are not the only factors controlling tube growth.

Fig. 1. Transmitted-light photomicrograph of the lower half of specimen VIII-2A, annealed at 2.0 GPa and 1200 °C in the presence of CO_2-H_2O for 14 d. Scale bar = 1 mm. Tubes (etch tunnels) and linear arrays of fluid inclusions emanate from the bottom of the olivine single crystal (just above the scale bar; the single crystal is in direct contact here with polycrystalline olivine) and extend in a radial fashion roughly parallel to [010]. Several of these linear arrays of fluid inclusions can be traced to tubes in the process of necking down. The dark horizontal lines are cracks produced during the quench.

Composition and phase state of fluids trapped as inclusions

The fluid-filled tubes and inclusions generally contain liquid CO_2, CO_2 vapor, and liquid H_2O (Roedder, 1965, 1984), consistent with the composition of fluids added to the charges (Fig. 4). Liquid CO_2 in these inclusions freezes and melts several degrees below that of pure CO_2 and hence must contain an impurity such as CO, CH_4, or H_2. At least three different types of solid phases in the fluid inclusions have been identified by optical and micro-Raman studies: (1) an opaque platy mineral presumed to be graphite (Fig. 4a), (2) highly birefringent and sometimes radial fibrous masses of carbonate minerals, and (3) silicate material that is olivine crystallized on the inclusion walls of some samples and an amorphous film (glass?) in

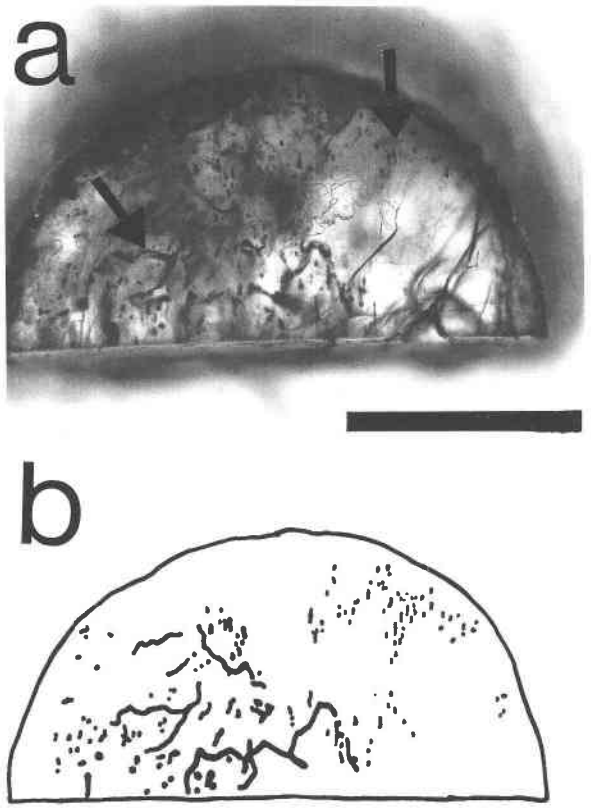

Fig. 2. (**a**) Transmitted-light photomicrograph of specimen IX-6 annealed at 3.0 GPa and 1200 °C for 2 d. Scale bar = 1 mm. The specimen was carefully removed intact from the Pt capsule, and the cylindrical crystal was cut in half lengthwise (i.e., parallel to [001] and normal to the polished flat ends). The bottom polished surface is facing the page. The sample was illuminated from below and obliquely from the sides. (**b**) Sketch shows the location of tubes and inclusions in **a**. Arrow on the left shows a tube (etch tunnel) roughly parallel to [001] that extends nearly 1 mm below the surface (i.e., into the page); it appears to merge with, or pass very close to, another tunnel. Several tubes extend into the crystal >0.5 mm. Arrow on the right shows droplet-shaped inclusions (elongated parallel to [100]) that represent healed tubes that originated from the circumference of the specimen. Note that a large region of the specimen on the right contains almost no inclusions or tubes.

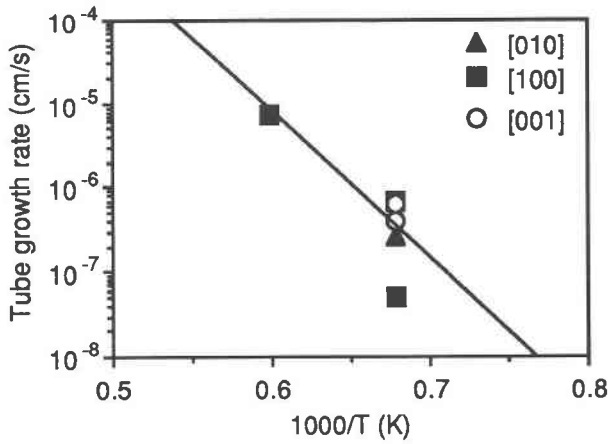

Fig. 3. Logarithm of the maximum growth rate of tubes (etch tunnels) vs. reciprocal temperature. Maximum growth rate was determined by measuring the length of the longest tube or linear fluid-inclusion array (since most tunnels were observed to be partially healed) and dividing by the experiment duration. The line is a visual best fit to the data and indicates that tube formation is thermally activated; the data are not sufficient to establish an Arrhenius relationship.

others (Fig. 4b, 4c). The relative proportions of phases among inclusion populations are highly variable.

Relation of tubes to dislocations

Specimen VIII-2A displayed both tubes and inclusions (Fig. 1). Part of the sample was subsequently heated in air at 900 °C for 20 min to oxidize the dislocation substructure near the surface (Kohlstedt et al., 1976). Oxidized dislocations are visible as dark reddish lines owing to the precipitation of very fine platelets of hematite. The oxidized specimen (Figs. 5, 6) contained a large number of lines that are identifiable as slip dislocations (cf. Kohlstedt et al., 1976; Zeuch and Green, 1977; Jin et al., 1989). Subgrain boundaries composed of arrays of these dislocations are also present, but neither tubes nor inclusions are associated with these dislocations. Curvilinear dislocations connecting inclusions in linear arrays (Fig. 5) and sometimes to tubes (Fig. 6) were also observed.

The lines that connect inclusions are distinctly more oxidized than the slip dislocations, and their orientations, lengths, low density, and sporadic occurrence suggest to us that they are growth dislocations. The existence of such

Table 1. Experiment table for specimens with etch tunnels

Specimen	*P* (GPa)	*T* (°C)	*t* (h)	Oxalic acid (mg)	Silver oxalate (mg)	Graphite (mg)	Orientation (parallel to the core axis)	Maximum tube length (μm)
III-2B	2.03	1200	46.4	2.26	—	—	[100]	84
III-2C	2.07	1400	2.0	2.15	—	—	[100]	524
III-3C	2.03	1200	47.1	—	1.32	—	[100]	1117
VIII-2A	2.03	1200	336.0	2.00	—	—	[010]	3136
IX-3	2.03	1200	48.3	0.59	—	1.20	[001]	693
IX-5	3.00	1200	0	0.38	—	0.47	[001]	0
IX-6	2.95	1200	54.5	0.64	—	1.50	[001]	1230

dislocations prior to tube formation may have been a primary reason why tubes formed at all in these crystals, and for this reason, it is important to determine if these dislocations existed prior to the high-temperature anneal. If the tube formed in a perfect crystal and the healing or regrowth process introduced dislocations, then one would expect to find an even number of dislocations connecting inclusions because the Burgers' vectors of these grown-in dislocations would have to cancel. Alternatively, if a dislocation existed prior to tube formation, then one would expect to find an odd number of dislocations connecting the inclusions in a linear array.

In many cases, we observed an odd number (either 1 or 3) of dislocations connecting inclusions in a linear array, suggesting that a dislocation did exist prior to tube formation. However, it is apparent that all the dislocations in the vicinity of the regrown tube may not have been oxidized because of their position relative to the narrow zone of oxidation (≈ 2 μm), Fe loss adjacent to the tube, or exclusion during preparation of the petrographic section. Regions near the circumference and polished ends of the specimen did not oxidize, and the reason for this is the well-established loss of Fe to Pt capsules at high temperature in a fluid environment. Regions adjacent to the linear inclusion arrays in some cases also showed no oxidation, suggesting that fluid either circulated in the tubes and carried Fe away or that the fluid-filled tubes provided a high-diffusivity path for Fe loss to the capsule (Fig. 5).

Although the observations above support the existence of growth dislocations prior to tube formation, it should be noted that the radial pattern of tubes in VIII-2A (Fig. 1) may not be compatible with this interpretation. It would be fortuitous if this particular sample was cored so as to sample a radial array of growth dislocations. Perhaps the radial pattern reflects a temperature gradient in the sample during the experiment.

The fluid-filled tubes described here resemble etch tunnels in quartz produced by HF etching and hydrothermal annealing. In light of the possibility that the similarity of these two phenomena reflects a common mode of origin, etch tunnel formation in quartz is briefly summarized below.

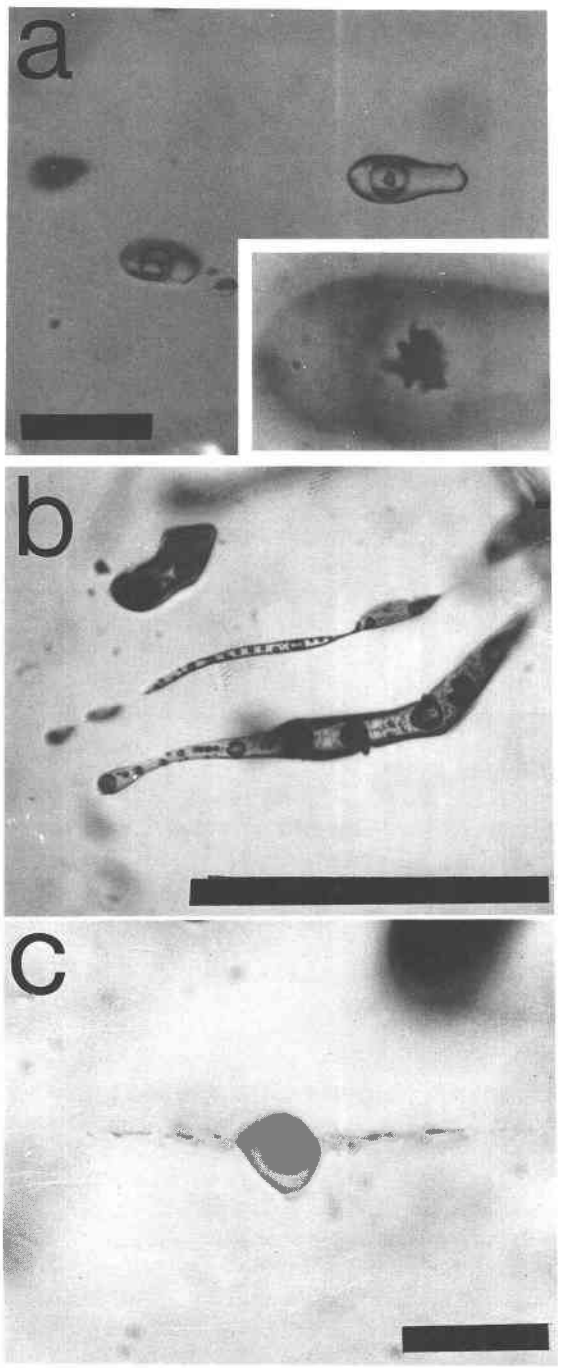

Fig. 4. (a) Photomicrograph (partially crossed polars) of H_2O-rich inclusions in sample III-3C, each with a bubble of high-pressure, dense CO_2. The larger inclusion also has a moveable cluster of opaque plates, visible in the enlargement shown in the inset. Scale bar = 20 μm. The presence of H_2O-rich inclusions in this sample (to which only CO_2 was added) is attributed to the diffusion of H (from the pressure assembly) into the Pt charge at high temperature and subsequent reaction with CO_2 to produce H_2O and CO or C. (b) Photomicrograph of tubular inclusions of silicate melt (?) with numerous bubbles in sample III-2C. Scale bar = 0.1 mm. (c) Photomicrograph of composite inclusion of high-pressure CO_2 and silicate melt (?) in sample IX-6 formed by healing of an etch tunnel. The horizontal crack represents partial decrepitation on pressure release during the quench. Scale bar = 20 μm.

Etch tunnel formation in quartz

Etch tunnels in quartz, commonly ribbon shaped, are about 1 μm across and show well-developed internal morphologies consistent with the known anisotropy of dissolution (Nielsen and Foster, 1960). Similarly, the growth rate of tunnels in quartz is anisotropic and may exceed 3 mm/d (Iwasaki, 1977). The majority of tubes are straight, but Hanyu (1964) has reported helical tubes.

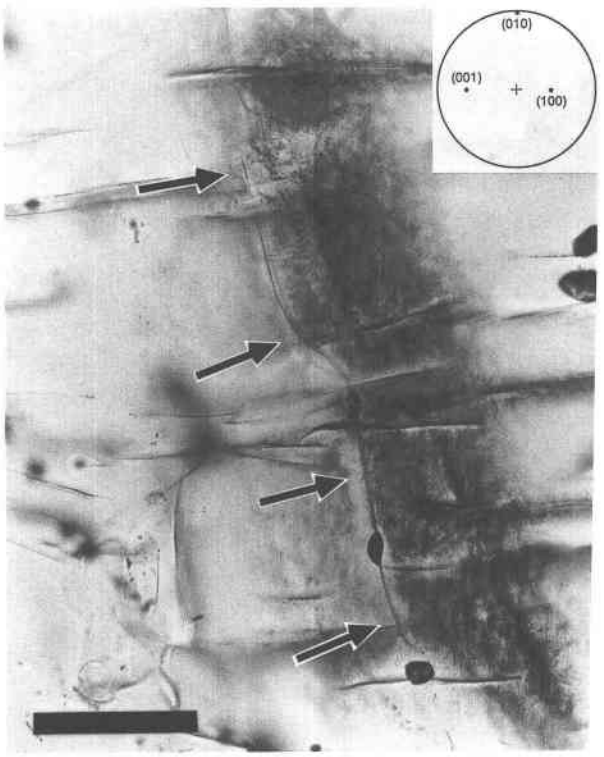

Fig. 5. Transmitted-light photomicrograph of VIII-2A after oxidation. Scale bar = 0.1 mm. The doubly polished section is approximately 60 μm thick. Oxidation of dislocations is confined to a narrow region (<10 μm) below the surface. Three inclusions are visible in the lower half of the photo; these represent a healed tube (etch tunnel) and are connected by straight and curvilinear dislocations, which have oxidized to produce the dark lines indicated by arrows. In the middle of the photomicrograph (second arrow from top), three dislocations can be discerned that extend and curve toward the top of the photo. One of those dislocations dips below the inclusion in the center, but it is out of focus and not visible. The dark region to the right of the linear inclusion array is hematite on the surface of the specimen and should be ignored. At the third arrow from the top, a lighter halo is visible around the dislocation connecting the two inclusions and represents Fe loss that has accompanied tube formation or healing.

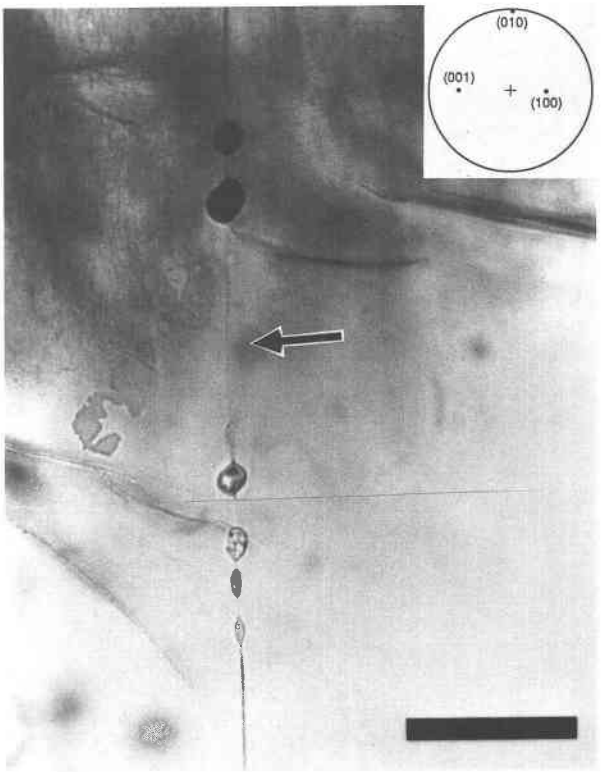

Fig. 6. Transmitted-light photomicrograph of VIII-2A after oxidation. Scale bar = 0.1 mm. A tube (etch tunnel) has been quenched in the process of necking down to form isolated inclusions. CO_2 vapor bubbles are visible in the inclusions. A faint line (arrow) representing an oxidized dislocation (parallel to [010]) connects the linear array of inclusions formed by the healing.

X-ray topography has demonstrated that etch tunnels in quartz form on dislocations with both edge- and screw-dominated components (Hanyu, 1964; Iwasaki, 1977). Carstens (1968) showed that etch tunnels were produced more readily in quartz crystals with high dislocation densities and high impurity contents.

Several ideas have been advanced to explain the formation of etch tunnels: (1) the crystal surface is "poisoned" (Brantley et al., 1986), (2) strain energy associated with the dislocation drives the dissolution and confines it to a narrow region (Iwasaki, 1977), (3) dissolution along dislocations is enhanced by the presence of an impurity (or impurities) segregated along the dislocation that increases the solubility of the crystal in the fluid.

Brantley et al. (1986) suggested that deep etch pits and etch tunnels might form if the crystal surface were "poisoned" such that continued dissolution of the crystal would occur only along dislocations intersecting the surface. Presumably the tube surfaces also would be poisoned, preventing their radial expansion and encouraging their elongation. Dissolution radially away from the dislocation core ultimately must be limited; otherwise the etched dislocations would be shaped like funnels and not tubes.

X-ray topographs of synthetic quartz crystals made before and after etching show that a small rotation of the lattice occurs in the vicinity of the etch tunnels. Iwasaki (1977) interpreted this as evidence for removal of the strained region, implying that the strained region around the dislocation localizes dissolution. Theoretical studies of etch pit formation that take into account the strain energy of the dislocation and the dislocation core seem to show that the strained region should not extend dissolution more than a few unit cells away from the core (Lasaga and Blum, 1986; Brantley et al., 1986), whereas etch tunnels are typically >1 μm in diameter.

Model 3 is the more commonly accepted origin for etch tunnels in quartz. Nielsen and Foster (1960) noted that

etch tunnels were more likely to form on faces known to contain the most impurities. They suggested that impurities (perhaps H) might diffuse to and precipitate on dislocations, thus making them more likely to dissolve. HF etching produces etch tunnels more readily in natural quartz with higher impurity contents than in quartz with low impurity contents (Carstens, 1968). Folk (1989) cites evidence that Al is the impurity in quartz that has segregated on growth dislocations that dissolve to produce etch tunnels.

Discussion

It is apparent that impurities on growth dislocations may have influenced the formation of etch tunnels in olivine. We suppose that impurities are present on growth dislocations in San Carlos olivine and that the impurities locally enhance the solubility of olivine in the fluid or lower the melting temperature of olivine in the presence of fluid. Etch tunnels (tubes) begin to form by dissolution or melting of olivine, and the fluid sequesters impurities and provides a high diffusivity pathway for homogenization with the fluid outside the crystal. Later, the tubes heal into linear arrays of bubbles, in order to minimize their surface energy, and trap the fluid.

The most reasonable interpretation of our fluid-inclusion data is that there were two immiscible fluids present during most of the experiments, a silicate-carbonate-rich melt and a CO_2-H_2O-rich fluid. Such a silicate-carbonate-rich melt could account for the mostly solid inclusions observed in III-3C and III-2B and also could yield some crystallization of olivine on the tube and inclusion walls, as has been observed. The large compositional variability of the inclusions is interpreted to be the result of trapping different amounts of two coexisting, compositionally different fluids in any given inclusion or of trapping of a fluid whose composition changed with time during tube boring and subsequent (or concurrent?) tube healing. In fact, both processes could have occurred.

Chemical environment and fluid speciation are important aspects of etch tunnel formation in olivine; etch tunnels formed only in samples annealed in the NaCl + BN pressure assemblies and not in the NaCl + pyrex + alumina assemblies. As stated earlier, the NaCl + BN assemblies stabilize at a much lower f_{O_2} than the NaCl + pyrex + alumina assemblies, and this would affect the chemical activity and speciation of the fluid. Additional experiments are needed to elucidate the role of chemical environment in etch tunnel formation.

If growth of etch tunnels occurs by dissolution of olivine in the fluid phase, it is difficult to reconcile the correlation of maximum tube length and experiment duration (Table 1) with the observation that all tubes show some evidence of healing. Longer tubes were produced by longer experiments, suggesting that tube formation continued throughout the experiment. This is an unexpected result if tube growth is controlled simply by dissolution of olivine because the fluid probably is saturated with dissolved solids within several minutes at these conditions (cf. Schneider and Eggler, 1986). That longer tubes were produced by longer experiments also suggests that tube healing occurred late in the experiment. The tubes appear to heal from their distal ends, ruling out the possibility that they heal behind themselves as they grow. Healing (necking down) of tubes into inclusions is consistent with the experiments of Wanamaker and Evans (1985) on diffusional crack healing in olivine; they noted that 1–6 d were required at 1200 °C to form an isolated inclusion from a tube. These kinetics are orders of magnitude too slow to support healing during the quench. The healing process could be enhanced by a drop in the solubility of olivine in the fluid during decompression, but it is unlikely that such a decrease in solubility could explain the difference between Wanamaker and Evans' (1985) kinetics and those necessary to explain tube healing as a quench phenomenon.

Hacker and Christie (1991) recently showed that altered plagioclase crystals in experimentally deformed amphibolites contain linear defects showing anomalous contrast in the TEM. During electron irradiation, these anomalous regions rapidly become amorphous and transform into tubes. They suppose that these anomalous defects were "silica-water-filled tubes" at the conditions of the experiment. They do not explicitly state whether the anomalous regions represent a quenched silicate melt with dissolved H_2O or an H_2O-rich fluid with dissolved silicate material. From the standpoint of etch tunnel formation, the distinction between aqueous melt or silicate-rich fluid may not be significant. The amphibolite is partially molten at the conditions of their experiments, and the altered plagioclase crystals (with variable and generally more calcic An contents than unaltered crystals) are probably those involved in the generation of melt. Although the dimensions of the tubes they observed in plagioclase are smaller than the etch tunnels in olivine described here, the processes by which they are produced may be quite similar. They consider these tubes to be a previously unrecognized mechanism of chemical transport.

If Hacker and Christie (1991) are correct that dissolution (or melting) of linear defects is a fundamental mechanism by which minerals approach equilibrium, then some of the questions left unanswered by this study warrant further investigation. For example, are impurities segregated on growth dislocations in San Carlos olivine, and if so, what are they and how do they influence dissolution and melting? Why is etch tunnel formation sensitive to the chemical environment stabilized by the pressure assembly? Most problematic of all, when do etch tunnels stop growing and start healing?

Finally, previous experiments with C-O-H fluids conducted in piston cylinder apparatus utilizing BN in the pressure assemblies probably have produced etch tunnels in minerals. Such fluid-filled tubes likely would have been interpreted as crystal growth phenomena by previous investigators; etch tunnels are observable in the polycrystalline olivine surrounding the single crystals in our experiments. If we had not been using large olivine single

crystals, it is not likely that we would have recognized etch tunnels in olivine either.

Acknowledgments

This research was made possible by grants from the National Science Foundation (EAR-8206915 and EAR-8418965) to H.W.G. and a Mineralogy-Petrology Research Award to T.N.T. from the Mineralogical Society of America. T.N.T. also acknowledges financial support from GRI research grant 5087-260-1626 while completing this work at Stanford University. Z. Jin advised us on oxidation decoration of dislocations in olivine, and Cheryl Knight performed the Raman studies. Critical comments to an earlier version of this manuscript by A. Blum and M. Hochella were greatly appreciated. The authors would like to thank J. Abril, L. Andersson, and N. Winter for their significant technical contributions to this study. Finally, we would like to thank I. MacInnis and P. Brown for their thoughtful, thorough, and constructive reviews.

References cited

Brantley, S.L., Crane, S.R., Crerar, D.A., Hellman, R., and Stallard, R. (1986) Dissolution at dislocation etch pits in quartz. Geochimica et Cosmochimica Acta, 50, 2349–2362.

Carstens, H. (1968) The lineage structure of quartz crystals. Contributions to Mineralogy and Petrology, 18, 295–304.

Folk, R.L. (1989) Internal structures of quartz revealed by boiling concentrated hydrofluoric acid. Journal of Geological Education, 37, 250–260.

Folk, R.L., Hoops, K., and Ide, S. (1987) Internal architecture of quartz revealed by SEM examination of HF-etched crystals. Bulletin of the Electron Microscopy Society of America, 17, 81.

Hacker, B.R., and Christie, J.M. (1991) Observational evidence for a possible new diffusion path. Science, 251, 67–70.

Hanyu, T. (1964) Dislocation etch tunnels in quartz crystals. Journal of the Physical Society of Japan, 19, 1489.

Iwasaki, F. (1977) Line defects and etch tunnels in synthetic quartz. Journal of Crystal Growth, 39, 291–298.

Jin, Z.-M., Green, H.W., and Borch, R.S. (1989) Microstructures of olivine and stresses in the upper mantle beneath eastern China. Tectonophysics, 169, 23–50.

Kohlstedt, D.L., Goetze, C., Durham, W.B., and Vander Sande, J.B. (1976) New technique for decorating dislocations in olivine. Science, 191, 1045–1046.

Lasaga, A.C., and Blum, A.E. (1986) Surface chemistry, etch pits and mineral reactions. Geochimica et Cosmochimica Acta, 50, 2363–2380.

Nielsen, J.W., and Foster, F.G. (1960) Unusual etch pits in quartz crystals. American Mineralogist, 45, 299–310.

Roedder, E. (1965) Liquid CO_2 inclusions in olivine-bearing nodules and phenocrysts in basalts. American Mineralogist, 50, 1746–1786.

——— (1984) Fluid inclusions. Mineralogical Society of America Reviews in Mineralogy, 12, 644 p.

Schneider, M.E., and Eggler, D.H. (1986) Fluids in equilibrium with peridotite minerals: Implications for mantle metasomatism. Geochimica et Cosmochimica Acta, 50, 711–724.

Tingle, T.N. (1987) An evaluation of the carbon-14 beta track technique: Implications for solubilities and partition coefficients determined by beta track mapping. Geochimica et Cosmochimica Acta, 51, 2479–2487.

——— (1988) Retrieval of uncracked single crystals from high pressure in piston-cylinder apparatus. American Mineralogist, 73, 1195–1197.

Tingle, T.N., Green, H.W., and Finnerty, A.A. (1988) Experiments and observations bearing on the solubility and diffusivity of carbon in olivine. Journal of Geophysical Research, 93, 15289–15304.

Wanamaker, B.J., and Evans, B.L. (1985) Experimental diffusional crack healing in olivine. In R.N. Schock, Ed., Point defects in minerals, Geophysical Monograph Series, 31, p. 194–210. American Geophysical Union, Washington, DC.

Wendlandt, R.F., Huebner, J.S., and Harrison, W.J. (1983) The redox potential of boron nitride and implications for its use as a crucible in experimental petrology. American Mineralogist, 65, 37–44.

Zeuch, D.H., and Green, H.W. (1977) Naturally decorated dislocations in olivine from peridotite xenoliths. Contributions to Mineralogy and Petrology, 62, 141–151.

Manuscript received September 6, 1990
Manuscript accepted November 5, 1991